



## Cold plasma-treated medium preferentially eliminates doxorubicin-resistant osteosarcoma cells

Juan Tornín<sup>a,b,\*\*\*</sup>, Borja Gallego<sup>a,b</sup>, Verónica Rey<sup>a,b,c</sup>, Dzohara Murillo<sup>a,b</sup>, Carmen Huergo<sup>a,b</sup>, Aida Rodríguez<sup>a,b</sup>, Cristina Canal<sup>d,e,f,\*\*</sup>, René Rodríguez<sup>a,b,c,\*</sup>

<sup>a</sup> Sarcomas and Experimental Therapeutics Laboratory, Instituto de Investigación Sanitaria del Principado de Asturias (ISPA), Hospital Universitario Central de Asturias, Avenida de Roma, s/n, 33011, Oviedo, Spain

<sup>b</sup> Instituto Universitario de Oncología del Principado de Asturias, 33011, Oviedo, Spain

<sup>c</sup> CIBER en oncología (CIBERONC), 28029, Madrid, Spain

<sup>d</sup> Biomaterials, Biomechanics and Tissue Engineering Group, Materials Science and Engineering Department, Research Center for Biomedical Engineering, Universitat Politècnica de Catalunya-BarcelonaTECH (UPC), Escola d'Enginyeria Barcelona Est (EEBE), C/Eduard Maristany 14, 08019, Barcelona, Spain

<sup>e</sup> Institut de Recerca Sant Joan de Déu, 08034, Barcelona, Spain

<sup>f</sup> Barcelona Research Center in Multiscale Science and Engineering, UPC, 08019, Barcelona, Spain

### ARTICLE INFO

#### Keywords:

Osteosarcoma  
Cold atmospheric plasma  
Oxidative stress  
Doxorubicin  
Drug-resistance

### ABSTRACT

Osteosarcoma (OS) is an aggressive bone cancer with poor prognosis, largely due to the limited effectiveness of current treatments such as doxorubicin (DX). Developing ways to overcome DX resistance is a significant clinical challenge. Here, we used two DX-resistant models to study the potential of Cold Plasma Treated Medium (PTM) to prevent DX resistance in OS. During the acquisition of the resistant phenotype upon long-term DX exposure, OS resistant cells became less proliferative, overexpressed the drug resistance-related efflux pump MDR1 and displayed a concomitant loss of SOD2 or GPX1. According to the reduced expression of these antioxidant enzymes, PTM treatment produced higher levels of oxidative stress and was more effective in eradicating DX-resistant cells. Moreover, PTM reduced the expression of MDR1, thus sensitizing resistant cells to DX. These findings uncover new vulnerabilities of DX-resistant cells related with their inability to cope with excessive oxidative stress and their dependence on MDR1 that can be exploited using PTM-based treatments to provide new therapeutic approaches for the management of drug resistance in OS.

### 1. Introduction

Osteosarcoma (OS) is a type of primary bone tumor that mainly affects children and young adults [1,2]. Although the cornerstone of OS management is the wide margin surgical resection of the primary tumor, adjuvant chemotherapy and/or irradiation are often employed for unresectable or metastatic tumors [3,4]. Unfortunately, traditional therapies frequently fail due to the development of resilient tumor subclones, resulting in more than 30 % of localized OS patients and more than 80 % of metastatic or refractory cases succumbing to the disease [5,

6]. Among traditional chemotherapeutic agents, Doxorubicin (DX) is one of the most widely used for OS therapy [1,4]. DX is an anthracycline drug that induces cancer cell death via nuclear and mitochondrial DNA intercalation, topoisomerase II inhibition, cytochrome *c* release from mitochondria, and generation of secondary reactive oxygen species (ROS) leading to oxidative stress and apoptosis induction [7]. However, the clinical application of DX is limited by its insufficient efficacy and severe side effects on healthy tissues [8].

Cold Atmospheric Plasma (CAP) is emerging as a promising non-invasive and pro-oxidant therapy for cancer [9,10]. As the fourth state of matter, CAP is formed by applying an electrical discharge to a gas to

\* Corresponding author. Sarcomas and Experimental Therapeutics Lab., Instituto de Investigación Sanitaria del Principado de Asturias (ISPA), Av. de Roma s/n, 33011, Oviedo, Spain.

\*\* Corresponding author. Biomaterials, Biomechanics and Tissue Engineering Group, Dpt. Materials Science and Engineering and Research Center for Biomedical Engineering, Universitat Politècnica de Catalunya-BarcelonaTECH (UPC), Escola d'Enginyeria Barcelona Est (EEBE), c/ Eduard Maristany 14, 08019, Barcelona, Spain.

\*\*\* Corresponding author. Sarcomas and Experimental Therapeutics Lab., Instituto de Investigación Sanitaria del Principado de Asturias (ISPA), Av. de Roma s/n, 33011, Oviedo, Spain.

E-mail addresses: [juantornin@ispasturias.es](mailto:juantornin@ispasturias.es) (J. Tornín), [cristina.canal@upc.edu](mailto:cristina.canal@upc.edu) (C. Canal), [rene.rodriguez@ispasturias.es](mailto:rene.rodriguez@ispasturias.es) (R. Rodríguez).

<https://doi.org/10.1016/j.freeradbiomed.2023.10.394>

Received 16 August 2023; Received in revised form 11 October 2023; Accepted 13 October 2023

Available online 14 October 2023

0891-5849/© 2023 The Authors. Published by Elsevier Inc. This is an open access article under the CC BY-NC license (<http://creativecommons.org/licenses/by-nc/4.0/>).

### Abbreviations

APPJ	Atmospheric Pressure Plasma Jet
DX	Doxorubicin
DX-R	Doxorubicin resistant cells
CAP	Cold Atmospheric Plasma
CAT1	Catalase 1
GPX1	Glutathion Peroxidase 1
OCT4	Octamer-binding transcription factor 4
OS	Osteosarcoma
PTL	Cold-Plasma Treated Liquids
PTM	Cold-Plasma Treated Medium
RONS	Reactive Oxygen and Nitrogen Species
SOD2	Superoxide Dismutase 2
UV	Ultraviolet radiation

partially or fully ionize it while keeping the temperature low enough to enable its application to living tissues and cells. CAP contains various components such as photons, electrons, ions, neutral radicals, including Reactive Oxygen and Nitrogen Species (RONS), ultraviolet (UV) and visible light, and electromagnetic fields. Studies have shown that CAP therapies selectively eliminate cancer cells while leaving healthy cells unharmed [11,12]. In recent years, CAP has garnered attention due to its ability to reverse drug-resistant properties in various tumor types like pancreatic cancer [13], glioma [14] and others [15]. However, its effectiveness against drug resistance in osteosarcoma (OS) remains unexplored.

Furthermore, while direct CAP treatment through endoscopy is under investigation for certain internal cancer [16,17], it is important to note that this approach is not currently available for OS. The unique challenges associated with treating OS have prompted alternative strategies, such as the development of Cold Plasma-Treated Liquids (PTLs), which are being actively explored as delivery systems of cold-plasma derived RONS. PTLs allow for the accumulation of the most relevant RONS from CAP and may be locally delivered to the tumor site using minimally invasive approaches like injection [18,19]. PTLs are obtained by applying CAP to a liquid or hydrogel to obtain a liquid vehicle that incorporates the long-lived RONS produced by CAP, such as H<sub>2</sub>O<sub>2</sub> or NO<sub>2</sub><sup>-</sup>, among others [10]. These PTLs have shown great activity against osteosarcoma using various liquids as cell culture medium [11,20] or Ringer's saline solutions [18,21,22].

Previous studies have shown that the anti-tumoral selectivity of PTLs against primary bone cancers is modulated by various factors such as the type of plasma device, time, cell surface, well-plate, volume of liquid, and overall biochemical composition of the liquid [10,11,22–24]. Notably, the use of Plasma Treated cell culture Medium (PTM) has been shown to increase the cytotoxic potential of DX against metastatic prostate cancer [25], and the combination of low dose PTL with low dose DX selectively eliminated cancer cells while leaving healthy counterparts unaffected.

Drug resistance is a major obstacle in the treatment of osteosarcoma (OS), so in light of the previous findings, it is the aim of this study to investigate whether cold plasma-treated medium (PTM) may be employed as a strategy to overcome DX resistance in OS. It is our hypothesis that PTM may sensitize DX-resistant OS cells to the drug. To verify this hypothesis, we employed PTM generated at different treatment times to challenge the DX-resistant phenotype in OS cells and investigate the molecular mechanisms involved in the observed cytotoxic effects.

## 2. Materials and methods

### 2.1. Cell culture and drugs

Two human osteosarcoma cell lines, 143.B (CRL-8303TM) and SaOS-2 (HTB-85TM), and their respective DX-resistant cell lines (143.B/DX-R and SaOS-2/DX-R), were used in this study. The DX-resistant cell lines were generated by exposing the parental cell lines to several rounds of stepwise increasing concentrations of DX using a previously established protocol [26]. Both, parental and DoxR cell lines were cultured at 37 °C in a humidified atmosphere containing 5 % CO<sub>2</sub> in McCoy medium supplemented with 10 % fetal bovine serum and penicillin/streptomycin (50 U/mL and 50 µg/mL, respectively), all of which obtained from GibcoTM (Carlsbad, CA, USA). Cell cultures were tested regularly to detect mycoplasma contamination using the Biotools Mycoplasma Gel Detection kit (B&M LABS, Madrid, Spain). DX was purchased from Selleckchem (Houston, TX, USA) and stored as 10 mM solutions in sterile DMSO at –80 °C. The drug was diluted in culture medium to the final concentration just before use.

### 2.2. Cytotoxic assays

Cell viability was assayed using the cell proliferation reagent WST-1 (Roche Mannheim, Germany) as previously described [9]. The surviving fraction and the IC<sub>50</sub> values were determined using GraphPad Prism 9.0.1 software (Graphpad Software Inc., San Diego, CA, USA) [27]. Resistance index (RI) for DX-resistant cell lines was calculated as the ratio of the IC<sub>50</sub> values of the cells the resistant models treated with DX or DX + PTM-30s to the IC<sub>50</sub> of the corresponding parental line treated with DX. Additionally, the effect of PTM on the proliferation ability of OS cells was analyzed using the xCELLigence system (ACEA Biosciences, Inc, San Diego, CA, USA). A suspension of 2 × 10<sup>3</sup> of 143.B or 1 × 10<sup>4</sup> of SaOS-2 cells in 500 µL of culture medium were seeded in specially designed microtiter plates containing interdigitated gold microelectrodes. After 24 h of cell seeding, 400 µL of culture medium was replaced with 400 µL of PTM treated for 30s. Real-time proliferation, measured as cell impedance changes (cell index), was monitored by the xCELLigence system every hour until the end of experiment (160 h) [18,28].

### 2.3. Intracellular ROS

Intracellular levels of ROS were measured using Peroxy Orange 1 (PO1) Bio-Techne R&D Systems, Minneapolis, MN, USA). Osteosarcoma (OS) cells were seeded into a dark 96-well plate at a density of 20 × 10<sup>3</sup> cells per 100 µL of culture medium. The following day, the culture medium was substituted with 100 µL of fresh culture media containing 10 µM of PO1 (Stock 10 mM in DMSO), and the cells were incubated for 60 min under standard cell culture conditions. After that, cells were gently washed with 1x DPBS to remove any residual probe, and the cell culture medium was replaced with 100 µL of PTM – 30 s or untreated cell culture as control. Subsequently, the intracellular fluorescence intensity was measured using a Synergy HTX Hybrid Multi-Mode Microplate Reader, with excitation at λ<sub>ex</sub> = 530/20 nm and emission at λ<sub>em</sub> = 590/20 nm as the excitation and emission wavelength filters, respectively. To calculate the intracellular production of H<sub>2</sub>O<sub>2</sub>, the increase in fluorescence in PTM treated cells was compared to untreated cells, in both conditions the fluorescence signal from cells that were not incubated to PO1 served as background.

### 2.4. Cold Plasma Treated Medium (PTM)

The study utilized an atmospheric pressure plasma jet (APPJ) with Helium (5.0 Linde, Spain) to generate plasma-treated medium (PTM). The APPJ has a single electrode configuration, and its details are described elsewhere [11]. A high voltage power supply from Conrad Electronics, consuming 6 W of nominal power, energized the electrode

with a sinusoidal waveform at 25 kHz. This generated a discharge with an applied voltage (U) of approximately 2 kV and a discharge current (I) of approximately 3 mA. The flow of Helium in the capillary was regulated at 1 L/min using a MassView flow controller (Bronkhorst, Netherlands). To generate the PTM, 0.5 mL of McCoy medium in a 24-well plate was exposed to the APPJ under the following conditions: 1) Helium flow rate of 1 L/min, 2) 10 mm gap between the plasma jet nozzle and the liquid surface, and 3) treatment time ranging from 5 to 480 s. The PTM is added to the cell cultures as rapidly as possible, typically within a time frame of 5 min, to ensure the maintenance of RONS during cell exposure.

### 2.5. Concentration of RONS in PTM

Here, we analyzed the concentration of two of the long-lived RONS generated in the liquid by the plasma treatment and more studied in the field: Nitrites and hydrogen peroxide. The determination of  $\text{NO}_2^-$  was performed using the Griess reagent and the concentration of  $\text{H}_2\text{O}_2$  was determined by Amplex™ Red Hydrogen/HRP Peroxide Kit (cat.no A2218, Invitrogen) according to a previous protocol [10].

### 2.6. Western blotting

Protein extraction was performed using a previously described protocol [10]. Briefly,  $1 \times 10^6$  cells were cultured in P100 dishes, and after 24 h, the cell culture medium was replaced with 8 mL of PTM and/or DX and incubated for different times. The cells were then recovered by scraping in DPBS, and the cell extracts were lysed using M-PER (Thermo Scientific, Rockford, IL, USA) supplemented with Halt™ Protease Inhibitor Cocktail 100X (Thermo Scientific). The lysates were centrifuged, and the supernatants were collected. The protein concentration was quantified using the Bradford dye-binding method (Bio-Rad protein assay kit; Bio-Rad) and the SDS-PAGE procedure were described elsewhere [29]. The primary antibodies used were anti-ABCB1 [(13342), 1:1000 dilution] from Cell Signaling (Danvers, MA, USA); anti-GPX1 [(ab108427), 1:1000] from Abcam (Cambridge, UK); anti-CAT1 [(MAB4934), 1:1000] and anti-SOD2 [(MAB3419), 1:2000] from Proteintech (Manchester, UK); and anti- $\beta$ -Actin [(A5441), 1:10,000 dilution] from Sigma-Aldrich (St Louis, MO, USA). The IRDye infrared fluorescent secondary antibodies IRDye 800CW and IRDye-680RD from LI-COR Biosciences (Lincoln, NE) (1:10,000) were used for signal detection using an Odyssey Fc imaging system and the Image Studio software (LI-COR Biosciences).

### 2.7. Statistical analysis

Statistical analysis was performed using GraphPad Prism version 8.0 (Graphpad Software Inc, La Jolla, CA, USA). Data are presented as the mean ( $\pm$  standard deviation, as indicated) of at least three independent experiments. Two-sided Student's *t*-test was performed to determine the statistical significance between groups.  $p < 0.05$  values were considered statistically significant.

## 3. Results

### 3.1. The higher sensitivity of DX-resistant cells to PTM is associated with increased intracellular ROS accumulation

To investigate the cytotoxic potential of PTM we treated cell culture media with APPJ operating at 1 L/min for different times to generate PTMs with increasing levels of RONS that were used to treat parental and DX-R OS cell lines (Fig. 1A). Among the various RONS formed by the APPJ in the cell culture medium, we focused on two relevant long-lived species [10], namely  $\text{H}_2\text{O}_2$  and  $\text{NO}_2^-$ . The concentration of both  $\text{NO}_2^-$  (Fig. 1B) and  $\text{H}_2\text{O}_2$  (Fig. 1C) increased in a time-dependent manner upon exposure to CAP. We observed that at treatment times shorter than 30 s, PTM contained a balanced cocktail of nitrites and hydrogen peroxide (e.g., PTM - 30 s produced a ratio  $[\text{H}_2\text{O}_2]/[\text{NO}_2^-] = 1.5$  with  $33.07 \pm 5.63$   $\mu\text{M}$  of nitrites and  $51.15 \pm 9.06$   $\mu\text{M}$  of hydrogen peroxide), while treatment times exceeding 60 s produced a higher amount of hydrogen peroxide in all treatments (e.g., PTM - 480 s produced a ratio  $[\text{H}_2\text{O}_2]/[\text{NO}_2^-] = 4.6$  with  $131.5 \pm 37.29$   $\mu\text{M}$  of nitrites and  $599.15 \pm 204.95$   $\mu\text{M}$  of hydrogen peroxide) (Fig. 1B–C). It has been shown in previous works [11,18] that for treatments to target preferentially OS cell lines without affecting nonmalignant cells it is important to keep balanced ratios of these RONS.

Therefore, to evaluate the sensitivity of the DX-R models, we focused on treatments with a balanced ratio of RONS, obtained from shortly treated PTMs. We generated two Doxorubicin-resistant (DX-R) cell lines from SaOS-2 and 143.B by exposing the parental cell lines to increasing concentrations of DX, as described in the experimental part. Monolayer cultures of two human OS cell lines (143.B and SaOS-2) were treated with PTM generated after an exposure of 30 s to CAP (PTM - 30 s). The cytotoxic effects of the PTM treatments were then evaluated using the iCELLigence system (Fig. 2A–B). Our results showed that both DX-R cells exhibited lower proliferation rates than their parental counterparts in both cell lines. In the presence of PTM, the proliferation of the parental and DX-R cell lines was greatly inhibited. However, DX-R cells showed a

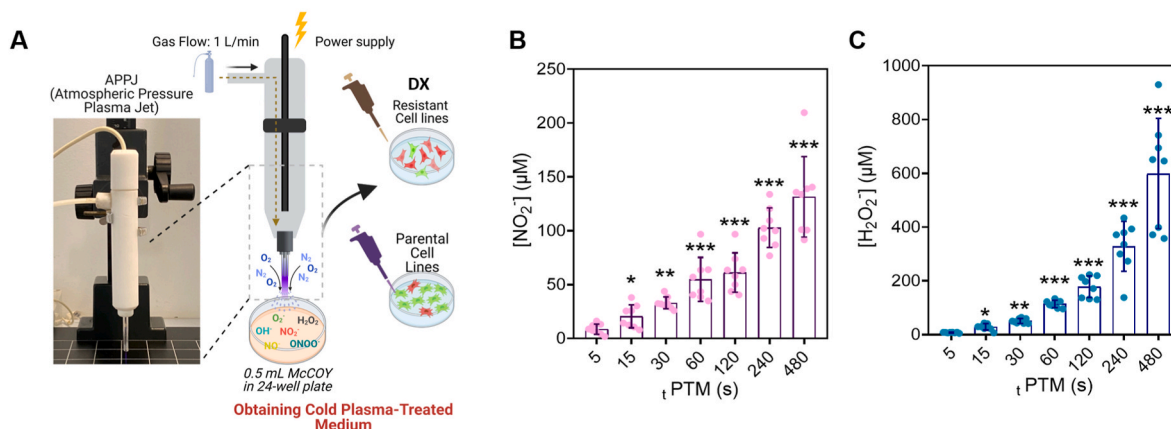


**Fig. 1. Plasma jet generates reactive species in the liquid phase.** (A) Schematic representation of the plasma jet (APPJ) used to treat McCoy cell culture medium to obtain PTM. An APPJ was used with 1 L/min of Helium on 0.5 mL of cell culture medium in 24-well plates. The APPJ was used to treat the cell culture medium for 5–480 s to obtain PTM with increasing levels of RONS. (B–C) The concentration of nitrites (B) and hydrogen peroxide (C) in the PTM was measured immediately after CAP treatment using untreated McCoy as a blank. Data are presented as the mean and error bars represent the SD ( $n = 8$ ). Asterisks indicate statistically significant differences with control untreated samples. (\*\*\* $p < 0.0005$ ; \*\* $p < 0.005$ ; \* $p < 0.05$ ; *t*-test). Scheme (A) was created using [biorender.com](https://www.biorender.com).

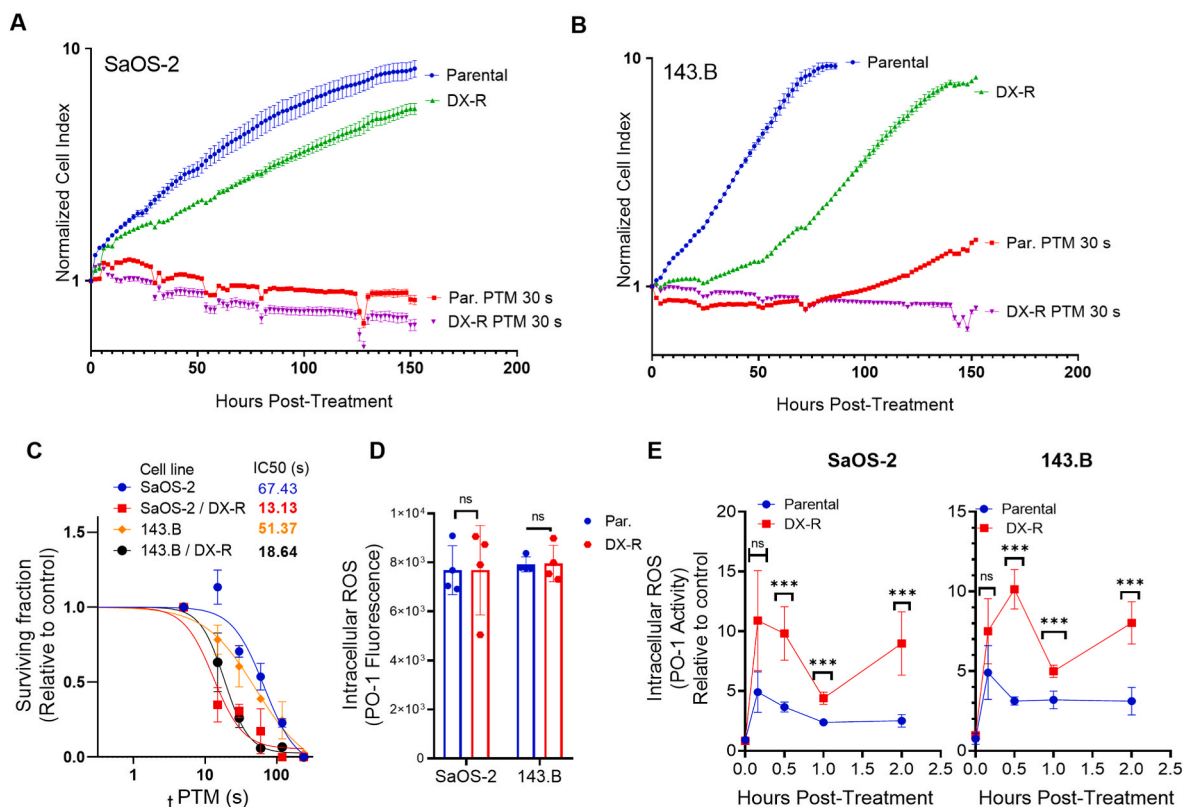


**Fig. 2.** Anti-proliferative effects of PTM in DX-R osteosarcoma cells. (A–B) Real-time proliferation (normalized cell index) was measured in SaOS-2 (A) and 143.B (B) cells treated or not with PTM – 30 s using an iCelligence system. Cell indices were normalized to the initial time ( $t = 0$ h). Data are presented as the mean and the SD of two biological replicates. Readings were done in duplicates using iCelligence. (C) Cell viability (WST-1 assay) of the indicated OS cell lines measured 72 h after the treatment with PTM exposed to CAP for increasing periods of time ( $t$  PTM (s)).  $IC_{50}$  values for each cell type are shown. Error bars represent the standard deviation of four independent experiments. (D–E) Intracellular cellular fluorescence of PO-1 was measured as an estimation of the intracellular ROS levels in control conditions (D) and at the indicated times after the exposure to PTM – 30 s (E). Values showed in (E) were relativized to the control (untreated) condition. Data are presented as the mean and standard deviation of  $n = 4$  replicates (\*\*\*)  $p$ -value  $< 0.005$ ; two-sided Student's  $t$ -test.

more durable response, since while the proliferation of the resistant models remained completely blocked 150 h after the start of the treatment, 143.B parental cells resumed proliferation after 60 h (Fig. 2B).

To better establish the response of parental and DX-R cell models to PTM, we performed endpoint (72h) dose-response viability assays by exposing cells to PTM generated after increasing treatment times up to 120 s (Fig. 2C). In these experiments, we observed that 143.B/DX-R and SaOS-2/DX-R cells showed  $IC_{50}$  values three to five times lower than those of their parental counterparts, respectively (Fig. 2C).

The cytotoxic effect of PTM has been widely attributed to the induction of intracellular oxidative stress [30,31]. To further investigate the specific vulnerabilities of DX-R cells to PTM, we analyzed the intracellular accumulation of ROS in both untreated cells and following PTM treatment. Although at basal levels, there were no observable differences in the accumulation of basal oxidative stress, (Fig. 2D), the treatment with PTM – 30 s led to a faster and more robust increase in intracellular ROS levels in DX-R cells compared to parental cells (Fig. 2E). These results suggest that the higher sensitivity of DX-R cells to PTM may be attributed to an increased accumulation of intracellular ROS in these models comparing to the corresponding parental cell lines.

### 3.2. Defective expression of antioxidant factors contributes to the higher sensitivity of DX-R cells to PTM treatment

Next, we aimed to study the mechanisms underlying the increased sensitivity of DX-R OS cells to PTM. For this purpose, we analyzed the effects of the acquisition of doxorubicin resistance after long-term exposure to this drug on the antioxidant machinery of OS cells. As

suitable models for this analysis, we used the entire collection of the stepwise-generated 143.B and SaOS-2 resistant models, in which, cells sequentially gained resistance to doxorubicin upon exposure to several rounds of increasing concentrations of DX (from  $IC_{20}$  to up  $128 \times IC_{20}$ ) [26]. In these models, we investigated the expression of Glutathione Peroxidase-1 (GPX1), mitochondrial Superoxide dismutase (SOD2), and Catalase 1 (CAT1), which are relevant anti-oxidant enzymes that scavenge the excess of RONS from cells and their expression may predict the response of tumor cells to PTM [18]. In addition, we analyzed the protein levels of the Multidrug Resistance Protein 1 (MDR1/ACBB1/P-gp), an efflux pump commonly associated to drug-resistant phenotypes [5] (Fig. 3A–C).

As expected, during the acquisition of the resistant phenotype we observed a large upregulation of MDR1, which was evident following the long-term exposure of OS cells to doxorubicin concentrations of  $4 \times IC_{50}$  or higher (Fig. 3A–C). In contrast, the levels of GPX1 and SOD2 were rapidly downregulated following continuous exposure to doxorubicin in both 143.B and SaOS-2 models. Differently, CAT1 levels were mostly unaffected during the chronic exposure to DX in both cell types (see Fig. 3A–C). This defective antioxidant phenotype may explain the higher levels of intracellular ROS observed in DX-R cells (Fig. 2D).

To further analyze the role of the modulation of antioxidant factors, we examined the evolution of the levels of CAT1, GPX1 and SOD2 following the treatment with PTM – 30 s (Fig. 3D). We found that, PTM did not induce a significant upregulation of any of these factors in neither of the DX-R models and their levels remain much lower than those observed in parental cells after 72 h of exposure to PTM (Fig. 3D–F).

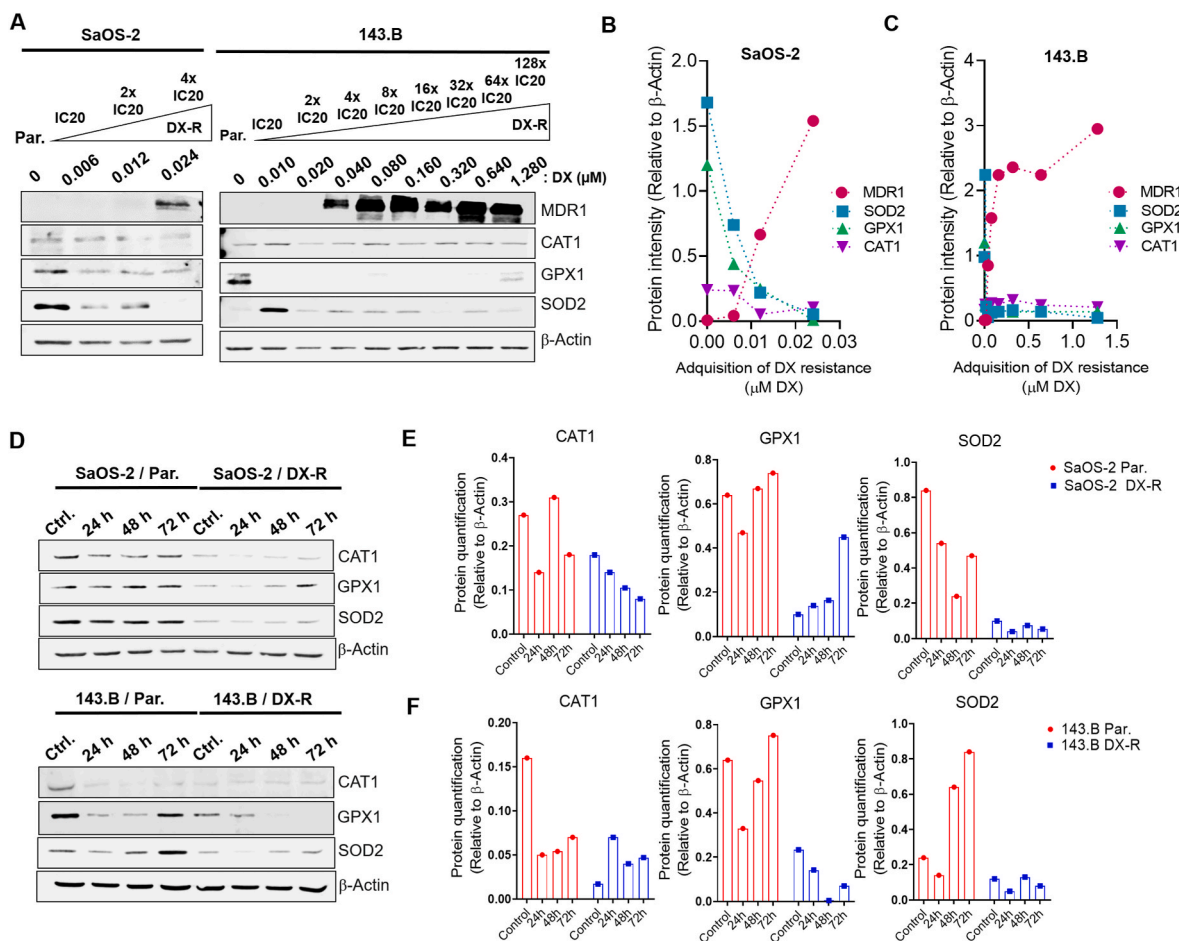


**Fig. 3. Modulation of the expression of antioxidant factors in OS cells during the acquisition of resistance to DX.** (A) Western blotting analysis of MDR1, SOD2, CAT1 and GPX1 levels in parental (par.) and stepwise-generated Saos2 (left panel) and 143B (right panel) DX-R models. These collections of increasingly-resistant cells were generated by exposure to sequential one-month treatments with step-by-step increased concentrations of DX. Cells were initially exposed to their corresponding IC20 and this concentration was doubled at each step until the maximum level of DX tolerance was reached. (B–C) Quantification of the indicated protein signal relative to  $\beta$ -actin levels in SaOS-2 (B) and 143-B (C) DX-R cells as a function of the concentration of DX used to obtain each increasingly resistant model of the collection. (D) Western blotting analysis of SOD2, CAT1 and GPX1 levels in parental (par.) and fully-resistant (DX-R) SaOS-2 (top panel) and 143B cells (bottom panel) after treatment with PTM – 30 s for 24, 48, or 72 h. (E–F) Quantification of the indicated protein signal relative to  $\beta$ -actin levels in SaOS-2 (E) and 143-B (F).  $\beta$ -Actin levels were used as a loading control in all Western blotting experiments.

Overall, these results suggest that acquisition of the DX-resistant phenotype leads to a decrease of the antioxidant defenses in OS cells which may potentially sensitize tumor cells to pro-oxidant therapies.

### 3.3. PTM restores DX sensitivity in OS DX-R cells

Finally, we evaluated the potential of PTM to increase the sensitivity to DX in parental and DX-R OS cells. In these experiments, we assessed the cell viability of cells treated with DX alone or in combination with PTM – 30 s. As expected, SaOS-2 and 143-B DX-R models exhibited IC<sub>50</sub> values approximately 60 times higher than the corresponding parental cells. Notably, PTM treatment was able to increase the cytotoxic effect of DX in parental cells, reducing IC<sub>50</sub> from 0.04 to 0.002  $\mu$ M in SaOS-2 cells and from 0.07 to 0.003  $\mu$ M in 143.B cells (Fig. 4A). This trend was also observed in DX-R models, in which the combination with PTM boosted the cytotoxic potential of DX both in SaOS-2/DX-R (IC<sub>50</sub> for DX: 2.76  $\mu$ M; IC<sub>50</sub> for DX + PTM: 0.97  $\mu$ M) and 143.B/DX-R cells (IC<sub>50</sub> for DX: 4.33  $\mu$ M; IC<sub>50</sub> for DX + PTM: 0.14  $\mu$ M) (Fig. 4A). According to these values, the combination of PTM and DX produced a large reduction of the DX resistance index in both models of DX-R cells (Fig. 4B).

To gain insights in the mechanism by which PTM enhances the anti-tumor activity of DX, we analyzed the protein levels of MDR1 in time-course and dose-response experiments. First, we found that PTM – 30

s induces a slight time-dependent downregulation of MDR1 in Saos2/DX-R and 143B/DX-R cells (Fig. 3C–D). Furthermore, a 24 h-treatment with a higher dose of PTM – 60 s produced a marked downregulation of the levels of this pro-resistant factor in both DX-R models, while this treatment did not induce MDR1 expression in parental cell lines (Fig. 4E–F). These results suggest that PTM may be a potential strategy to abrogate the expression of ABC pumps, such as MDR1, in OS cells, thereby enhancing DX efficacy.

## 4. Discussion

DX is the chemotherapeutic drug most commonly used to treat OS [1, 4]. However, the emergence of tumor resistance to DX represents a major clinical challenge in the management of OS [5,21] and, therefore, great effort is being undertaken to develop therapies capable of overcoming DX resistance [32–35]. The primary anti-tumor activity of DX is mediated by its ability to induce DNA damage in cancer cells. In addition, the cytotoxic effects of DX are also mediated by its ability to generate ROS [8,36]. However, ROS levels have a dual role in cancer [37,38]. On the one hand, the altered metabolism of tumor cells produces an increase in ROS levels, which in turn promote cell survival, genetic instability and drug resistance. On the other hand, a dramatic increase in ROS levels may overwhelm the anti-oxidant defenses of the

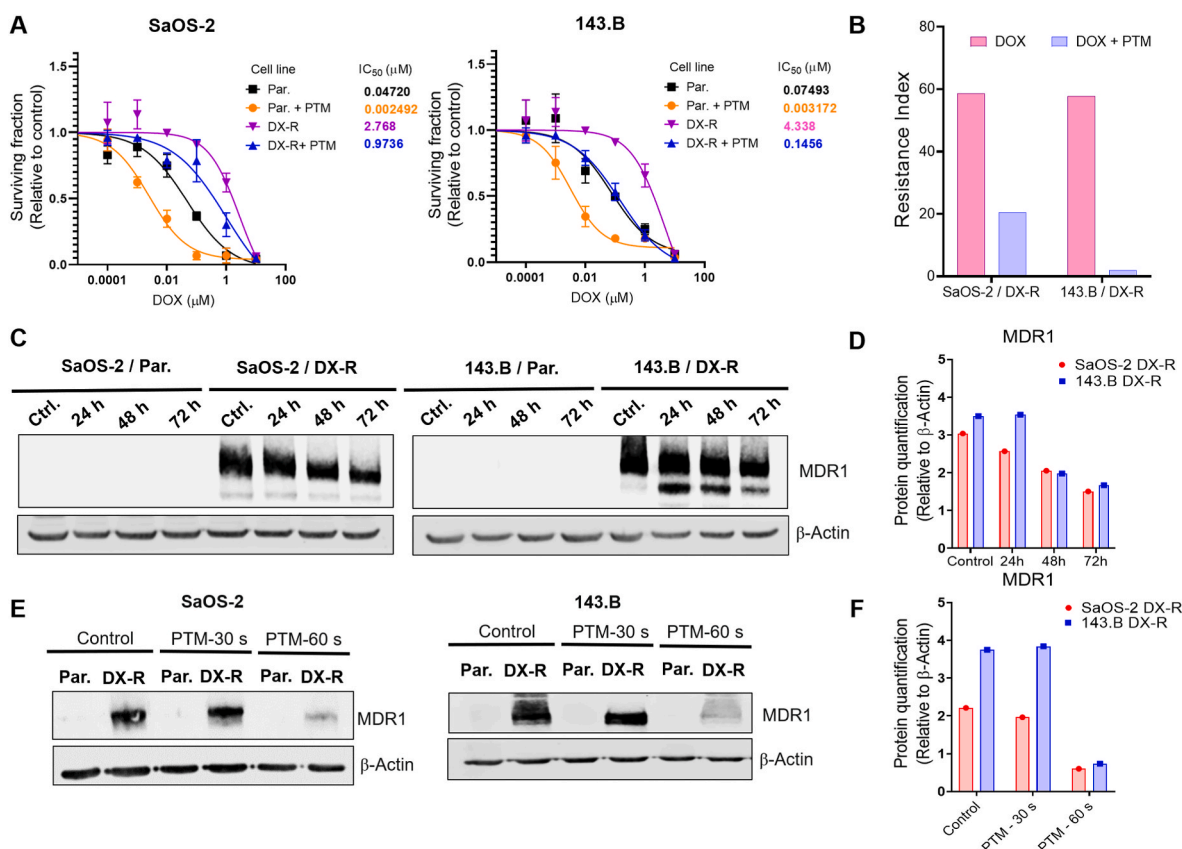


**Fig. 4. PTM restores DX sensitivity in DX-R cells.** (A) Cell viability was measured using WST-1 assay after treatment with increasing concentrations of DX alone or in combination with PTM-30s for 72 h in parental and DX-R cell lines. IC<sub>50</sub> values (μM) for each treatment are shown. Error bars represents the standard deviation of four independent experiments. (B) Resistance index (RI) for DX-resistant cell lines was calculated as the ratio of the IC<sub>50</sub> values of the cells the resistant models treated with DX or DX + PTM-30s to the IC<sub>50</sub> of the corresponding parental line treated with DX. (C–D) Western blotting analysis of MDR1 levels in parental (par.) and fully-resistant (DX-R) SaOS-2 (left panel) and 143B cells (right panel) after treatment with PTM – 30 s for 24, 48, or 72 h (C) and quantification of MDR1 protein signal relative to β-actin levels (D). (E–F) Western blotting analysis of MDR1 levels after exposing parental and DX-R SaOS-2 (left) and 143.B (right) cells to PTM generated by increasing exposure times to APPJ treatment for 24 h (E) and quantification of MDR1 levels relative to β-actin (F). β-Actin levels were utilized as the loading control in Western blotting experiments.

cancer cells, thus triggering cell death.

In this work, we found that OS cells react to long-term DX treatment by downregulating the expression of antioxidant enzymes. This may be a way of adapting to the ROS produced by DX, so that tumor cells ensure increased levels of ROS that can activate pro-resistance signaling. At the same time, this constitutes an opportunity to use pro-oxidant treatments capable of exceeding the threshold of resistance to ROS and eliminate DX-resistant populations. In this sense, CAP is pro-oxidant therapy which anti-tumor potential is being tested in clinical trials [39,40]. Relevantly, we have previously showed that PTL-based treatments exert a potent anti-tumor activity against OS cells both in vitro [10,11,22] and in vivo [18]. Here, we hypothesized that this treatment could also be effective against DX-R OS cells. Consistent with this assumption, we found that the exposure to PTM produced a higher level of ROS in DX-R cells compared to the corresponding parental models and this correlated with much lower survival of DX-R cells after the treatment. These results suggest that the downregulation of antioxidant enzymes detected in resistant cells represent a vulnerability to cope with sudden increases in intracellular ROS levels, and therefore PTM treatment is able to overwhelm the defenses of DX-R cells.

Previous findings also support the benefits of a combined treatment of DX and CAP-based therapies. First, it has been shown that direct CAP application increases the effectiveness of both free and liposomal DX in melanoma cancer cells [41]. Additionally, exposure to PTM promotes cell permeabilization and enhances DX uptake by HeLa Cells [42]. Likewise, we have shown that the combinatory treatment of DX and

PTLs increases the selective anti-cancer effect of DX in a metastatic prostate model [25]. The molecular basis of this synergy may be related with the reported ability of ROS to negatively regulate the expression of drug efflux pumps such as MDR1 when administrated at high levels [37, 43]. In line with this finding, we found that PTM downregulated the levels of MDR1 in a dose and time-dependent manner and accordingly co-treatment with PTM sensitized both parental and DX-R OS cells to the cytotoxic effect of DX. In any case, taking into account that parental cells do not express MDR1, there must be additional mechanisms involved in the synergistic effect of this combination.

### 5. Conclusion

This study reveals that during the process of gaining resistance to DX, OS cells acquire a defective antioxidant phenotype that can be exploited as vulnerability to the exposure to the high levels of ROS contained in PTLs. Moreover, PTM contribute to increase the anti-tumor potential of DX in a process related to their ability to regulate MDR1 levels. In summary, our study provides for the first time a rationale for the use of CAP-based treatments as way to overcome DX resistance in OS, thus supporting further studies aimed to evaluate the clinical efficacy of this approach.

### Author contributions

JT conceived the project, and designed experiments; JT, CH, VR, DM,

and BG performed experiments; JT, RR and CC wrote the manuscript. CC & RR contributed to the review of the manuscript; supervised the study & obtained funding.

### Declaration of competing interest

The authors declare no competing interest.

### Acknowledgements

This work was supported by the Agencia Estatal de Investigación (AEI) [MICINN/Fondo Europeo de Desarrollo Regional (FEDER) (grants PID2019-106666RB-I00 and PID2022-142020OB-I00 to R.R. and PID2019-103892RB-I00/AEI/10.13039/501100011033 to C.C.) and ISC III/FEDER (Consortio CIBERONC - CB16/12/00390]; the Plan de Ciencia Tecnología e Innovación del Principado de Asturias/FEDER [grant IDI/2021/000027 to R.R. and Severo Ochoa predoctoral fellowships BP-20-046 to B.G. and BP-21-084 to DM]; Fundación Científica de la Asociación Española Contra el Cáncer (AECC) (predoctoral fellowship to CH); CC belongs to SGR2022-1368 and acknowledges Generalitat de Catalunya for the ICREA Academia Award for Excellence in Research. We thank also COST Action CA20114 (Therapeutic Applications of Cold Plasmas) for the stimulating environment provided.

### References

- [1] T.G. Grunewald, M. Alonso, S. Avnet, A. Banito, S. Burdach, F. Cidre-Aranaz, G. Di Pompo, M. Distel, H. Dorado-García, J. García-Castro, L. González-González, A. E. Grigoriadis, M. Kasan, C. Koelsche, M. Krumbholz, F. Lecanda, S. Lemma, D. L. Longo, C. Madrigal-Esquível, A. Morales-Molina, J. Musa, S. Ohmura, B. Ory, M. Pereira-Silva, F. Perut, R. Rodríguez, C. Seeling, N. Al Shaaili, S. Shaabani, K. Shrivastava, S. Sinha, E.M. Tomazou, M. Trautmann, M. Vela, Y.M. Versluis-Jonkers, J. Visgauss, M. Zalacain, S.J. Schober, A. Lissat, W.R. English, N. Baldini, D. Heymann, Sarcoma treatment in the era of molecular medicine, *EMBO Mol. Med.* 12 (11) (2020), e11131, <https://doi.org/10.15252/emmm.201911131>.
- [2] R.D. Roberts, M.M. Lizardo, D.R. Reed, P. Hingorani, J. Glover, W. Allen-Rhoades, T. Fan, C. Khanna, E.A. Sweet-Cordero, T. Cash, M.W. Bishop, M. Hegde, A. R. Sertil, C. Koelsche, L. Mirabello, D. Malkin, P.H. Sorensen, P.S. Meltzer, K. A. Janeway, R. Gorlick, B.D. Crompton, Provocative questions in osteosarcoma basic and translational biology: a report from the Children's Oncology Group, *Cancer* 125 (20) (2019) 3514–3525, <https://doi.org/10.1002/ncr.32351>.
- [3] A.E. Badila, D.M. Radulescu, A.G. Niculescu, A.M. Grumezescu, M. Radulescu, A. R. Radulescu, Recent advances in the treatment of bone metastases and primary bone tumors: an up-to-date review, *Cancers* 13 (16) (2021), <https://doi.org/10.3390/cancers13164229>.
- [4] P.G. Casali, S. Bielack, N. Abecassis, H.T. Aro, S. Bauer, R. Biagini, S. Bonvalot, I. Boukovinas, J. Bovee, B. Brennan, T. Brodowicz, J.M. Broto, L. Brugieres, A. Buonadonna, E. De Alava, A.P. Dei Tos, X.G. Del Muro, P. Dileo, C. Dhooge, M. Eriksson, F. Fagioli, A. Fedenko, V. Ferraresi, A. Ferrari, S. Ferrari, A.M. Frezza, N. Gaspar, S. Gasperoni, H. Gelderblom, T. Gil, G. Grignani, A. Gronchi, R.L. Haas, B. Hassan, S. Hecker-Nolting, P. Hohenberger, R. Issels, H. Joensuu, R.L. Jones, I. Judson, P. Jutte, S. Kaal, L. Kager, B. Kasper, K. Kopeckova, D.A. Krakorova, R. Ladenstein, A. Le Cesne, I. Lugowska, O. Merimsky, M. Montemurro, B. Morland, M.A. Pantaleo, R. Piana, P. Picci, S. Piperno-Neumann, A.L. Pousa, P. Reichardt, M. H. Robinson, P. Rutkowski, A.A. Safwat, P. Schoffski, S. Sleijfer, S. Stacchiotti, S. J. Strauss, K. Sundby Hall, M. Unk, F. Van Coevorden, W.T.A. van der Graaf, J. Whelan, E. Wardelmann, O. Zaikova, J.Y. Blay, P. ESMO Guidelines Committee, E. Ern, Bone sarcomas: ESMO-PaedCan-EURACAN Clinical Practice Guidelines for diagnosis, treatment and follow-up, *Ann. Oncol.* : official journal of the European Society for Medical Oncology / ESMO 29 (Suppl 4) (2018) iv79–iv95, <https://doi.org/10.1093/annonc/mdy310>.
- [5] C.M. Hattinger, M.P. Patrizio, L. Fantoni, C. Casotti, C. Riganti, M. Serra, Drug resistance in osteosarcoma: emerging biomarkers, therapeutic targets and treatment strategies, *Cancers* 13 (12) (2021) 2878, <https://doi.org/10.3390/cancers13122878>.
- [6] S.T. Menéndez, B. Gallego, D. Murillo, A. Rodríguez, R. Rodríguez, Cancer stem cells as a source of drug resistance in bone sarcomas, *J. Clin. Med.* 10 (12) (2021) 2621, <https://doi.org/10.3390/jcm10122621>.
- [7] M. Kciuk, A. Gielecinska, S. Mujwar, D. Kolat, Z. Kaluzinska-Kolat, I. Celik, R. Kontek, Doxorubicin-an agent with multiple mechanisms of anticancer activity, *Cells* 12 (4) (2023), <https://doi.org/10.3390/10.3390/cells12040659>.
- [8] C. Carvalho, R.X. Santos, S. Cardoso, S. Correia, P.J. Oliveira, M.S. Santos, P. I. Moreira, Doxorubicin: the good, the bad and the ugly effect, *Curr. Med. Chem.* 16 (25) (2009) 3267–3285, <https://doi.org/10.2174/092986709788803312>.
- [9] A. Dubuc, P. Monsarrat, F. Virard, N. Merbahi, J.P. Sarrette, S. Laurencin-Dalieux, S. Cousty, Use of cold-atmospheric plasma in oncology: a concise systematic review, *Ther. Adv. Med. Oncol.* 10 (2018), 1758835918786475, <https://doi.org/10.1177/1758835918786475>.
- [10] J. Tornin, C. Labay, F. Tampieri, M.P. Ginebra, C. Canal, Evaluation of the effects of cold atmospheric plasma and plasma-treated liquids in cancer cell cultures, *Nat. Protoc.* 16 (6) (2021) 2826–2850, <https://doi.org/10.1038/s41596-021-00521-5>.
- [11] J. Tornin, M. Mateu-Sanz, A. Rodríguez, C. Labay, R. Rodríguez, C. Canal, Pyruvate plays a main role in the antimicrobial selectivity of cold atmospheric plasma in osteosarcoma, *Sci. Rep.* 9 (1) (2019), 10681, <https://doi.org/10.1038/s41598-019-47128-1>.
- [12] C. Canal, R. Fontelo, I. Hamouda, J. Guillem-Martí, U. Cvelbar, M.P. Ginebra, Plasma-induced selectivity in bone cancer cells death, *Free Radic. Biol. Med.* 110 (2017) 72–80, <https://doi.org/10.1016/j.freeradbiomed.2017.05.023>.
- [13] L. Brulle, M. Vandamme, D. Ries, E. Martel, E. Robert, S. Lerondel, V. Trichet, S. Richard, J.M. Povesles, A. Le Pape, Effects of a non thermal plasma treatment alone or in combination with gemcitabine in a MIA PaCa2-luc orthotopic pancreatic carcinoma model, *PLoS One* 7 (12) (2012), e52653, <https://doi.org/10.1371/journal.pone.0052653>.
- [14] J. Koritzer, V. Boxhammer, A. Schafer, T. Shimizu, T.G. Klampfl, Y.F. Li, C. Welz, S. Schwenk-Zieger, G.E. Morfill, J.L. Zimmermann, J. Schlegel, Restoration of sensitivity in chemo-resistant glioma cells by cold atmospheric plasma, *PLoS One* 8 (5) (2013), e64498, <https://doi.org/10.1371/journal.pone.0064498>.
- [15] D. Murillo, C. Huergo, B. Gallego, R. Rodríguez, J. Tornin, Exploring the use of cold atmospheric plasma to overcome drug resistance in cancer, *Biomedicines* 11 (1) (2023), <https://doi.org/10.3390/biomedicines11010208>.
- [16] E. Robert, M. Vandamme, L. Brullé, S. Lerondel, A. Le Pape, V. Sarron, D. Riès, T. Darny, S. Dozias, G. Collet, C. Kieda, J.M. Povesles, Perspectives of endoscopic plasma applications, *Clinical Plasma Medicine* 1 (2) (2013) 8–16, <https://doi.org/10.1016/j.cpm.2013.10.002>.
- [17] H. Decauchy, A. Pavy, M. Camus, L. Fouassier, T. Dufour, Cold plasma endoscopy applied to biliary ducts: feasibility risk assessment on human-like and porcine models for the treatment of cholangiocarcinoma, *J. Phys. Appl. Phys.* 55 (45) (2022), 455401, <https://doi.org/10.1088/1361-6463/ac8c4d>.
- [18] J. Tornin, M. Mateu-Sanz, V. Rey, D. Murillo, C. Huergo, B. Gallego, A. Rodríguez, R. Rodríguez, C. Canal, Cold plasma and inhibition of STAT3 selectively target tumorigenicity in osteosarcoma, *Redox Biol.* (2023), 102685, <https://doi.org/10.1016/j.redox.2023.102685>.
- [19] X. Sole-Martí, A. Espina-Noguera, M.P. Ginebra, C. Canal, Plasma-conditioned liquids as anticancer therapies in vivo: current state and future directions, *Cancers* 13 (3) (2021), <https://doi.org/10.3390/cancers13030452>.
- [20] T. Tokunaga, T. Ando, M. Suzuki-Karasaki, T. Ito, A. Onoe-Takahashi, T. Ochiai, M. Soma, Y. Suzuki-Karasaki, Plasma-stimulated medium kills TRAIL-resistant human malignant cells by promoting caspase-independent cell death via membrane potential and calcium dynamics modulation, *Int. J. Oncol.* 52 (3) (2018) 697–708, <https://doi.org/10.3892/ijo.2018.4251>.
- [21] M. Mateu-Sanz, J. Tornin, M.P. Ginebra, C. Canal, Cold atmospheric plasma: a new strategy based primarily on oxidative stress for osteosarcoma therapy, *J. Clin. Med.* 10 (4) (2021), <https://doi.org/10.3390/jcm10040893>.
- [22] M. Mateu-Sanz, J. Tornin, B. Brulin, A. Khluyustova, M.P. Ginebra, P. Layrolle, C. Canal, Cold plasma-treated Ringer's saline: a weapon to target osteosarcoma, *Cancers* 12 (1) (2020), <https://doi.org/10.3390/cancers12010227>.
- [23] A. Khluyustova, C. Labay, Z. Machala, M.-P. Ginebra, C. Canal, Important parameters in plasma jets for the production of RONS in liquids for plasma medicine: a brief review, *Front. Chem. Sci. Eng.* 13 (2) (2019) 238–252, <https://doi.org/10.1007/s11705-019-1801-8>.
- [24] J. Tornin, A. Villasante, X. Sole-Martí, M.P. Ginebra, C. Canal, Osteosarcoma tissue-engineered model challenges oxidative stress therapy revealing promoted cancer stem cell properties, *Free Radic. Biol. Med.* 164 (2021) 107–118, <https://doi.org/10.1016/j.freeradbiomed.2020.12.437>.
- [25] M. Mateu-Sanz, M.P. Ginebra, J. Tornin, C. Canal, Cold atmospheric plasma enhances doxorubicin selectivity in metastatic bone cancer, *Free Radic. Biol. Med.* 189 (2022) 32–41, <https://doi.org/10.1016/j.freeradbiomed.2022.07.007>.
- [26] B. Gallego, D. Murillo, V. Rey, C. Huergo, Ó. Estupiñán, A. Rodríguez, J. Tornin, R. Rodríguez, Addressing doxorubicin resistance in bone sarcomas using novel drug-resistant models, *Int. J. Mol. Sci.* 23 (12) (2022), <https://doi.org/10.3390/ijms23126425>.
- [27] L. Martínez-Cruzado, J. Tornin, A. Rodríguez, L. Santos, E. Allonca, M. T. Fernandez-García, A. Astudillo, J.M. García-Pedrero, R. Rodríguez, Trabectedin and camptothecin synergistically eliminate cancer stem cells in cell-of-origin sarcoma models, *Neoplasia* 19 (6) (2017) 460–470, <https://doi.org/10.1016/j.neo.2017.03.004>.
- [28] Ó. Estupiñán, V. Rey, J. Tornin, D. Murillo, B. Gallego, C. Huergo, V. Blanco-Lorenzo, M. Victoria González, A. Rodríguez, F. Moris, J. González, V. Ayllón, V. Ramos-Mejía, A. Bigas, R. Rodríguez, Abrogation of stemness in osteosarcoma by the mithramycin analog EC-8042 is mediated by its ability to inhibit NOTCH-1 signaling, *Biomed. Pharmacother.* 162 (2023), 114627, <https://doi.org/10.1016/j.biopha.2023.114627>.
- [29] P. Zuazua-Villar, R. Rodríguez, M.E. Gagou, P.A. Evers, M. Meuth, DNA replication stress in CHK1-depleted tumour cells triggers premature (S-phase) mitosis through inappropriate activation of Aurora kinase B, *Cell Death Dis.* 5 (5) (2014) e1253, <https://doi.org/10.1038/cddis.2014.231>.
- [30] P.M. Girard, A. Arbaban, M. Fleury, G. Bauville, V. Puech, M. Dutreix, J.S. Sousa, Synergistic effect of H2O2 and NO2 in cell death induced by cold atmospheric He plasma, *Sci. Rep.* 6 (2016), 29098, <https://doi.org/10.1038/srep29098>.
- [31] G. Bauer, D. Sersenova, D.B. Graves, Z. Machala, Cold atmospheric plasma and plasma-activated medium trigger RONS-based tumor cell apoptosis, *Sci. Rep.* 9 (1) (2019), 14210, <https://doi.org/10.1038/s41598-019-50291-0>.

- [32] L. Marchandet, M. Lallier, C. Charrier, M. Baud'huin, B. Ory, F. Lamoureux, Mechanisms of resistance to conventional therapies for osteosarcoma, *Cancers* 13 (4) (2021), <https://doi.org/10.3390/cancers13040683>.
- [33] R.A. Ward, S. Fawell, N. Floc'h, V. Flemington, D. McKercher, P.D. Smith, Challenges and opportunities in cancer drug resistance, *Chem. Rev.* 121 (6) (2021) 3297–3351, <https://doi.org/10.1021/acs.chemrev.0c00383>.
- [34] V. Hanusova, I. Bousova, L. Skalova, Possibilities to increase the effectiveness of doxorubicin in cancer cells killing, *Drug Metab. Rev.* 43 (4) (2011) 540–557, <https://doi.org/10.3109/03602532.2011.609174>.
- [35] O. Estupinan, L. Santos, A. Rodriguez, L. Fernandez-Nevaldo, P. Costales, J. Perez-Escuredo, M.A. Hermsilla, P. Oro, V. Rey, J. Tornin, E. Allonca, M.T. Fernandez-Garcia, C. Alvarez-Fernandez, A. Brana, A. Astudillo, S.T. Menendez, F. Moris, R. Rodriguez, The multikinase inhibitor EC-70124 synergistically increased the antitumor activity of doxorubicin in sarcomas, *Int. J. Cancer* 145 (1) (2019) 254–266, <https://doi.org/10.1002/ijc.32081>.
- [36] A. Korga, M. Ostrowska, M. Iwan, M. Herbet, J. Dudka, Inhibition of glycolysis disrupts cellular antioxidant defense and sensitizes HepG2 cells to doxorubicin treatment, *FEBS Open Bio* 9 (5) (2019) 959–972, <https://doi.org/10.1002/2211-5463.12628>.
- [37] S. Galadari, A. Rahman, S. Pallichankandy, F. Thayyullathil, Reactive oxygen species and cancer paradox: to promote or to suppress? *Free Radic. Biol. Med.* 104 (2017) 144–164, <https://doi.org/10.1016/j.freeradbiomed.2017.01.004>.
- [38] J.N. Moloney, T.G. Cotter, ROS signalling in the biology of cancer, *Semin. Cell Dev. Biol.* 80 (2018) 50–64, <https://doi.org/10.1016/j.semcdb.2017.05.023>.
- [39] J. Canady, S.R.K. Murthy, T. Zhuang, S. Gitelis, A. Nissan, L. Ly, O.Z. Jones, X. Cheng, M. Adileh, A.T. Blank, M.W. Colman, K. Millikan, C. O'Donoghue, K. M. Stenson, K. Ohara, G. Schtrechman, M. Keidar, G. Basadonna, The first cold atmospheric plasma phase I clinical trial for the treatment of advanced solid tumors: a novel treatment arm for cancer, *Cancers* 15 (14) (2023) 3688, <https://doi.org/10.3390/cancers15143688>.
- [40] Canady Helios Cold Plasma Scalpel Treatment at the Surgical Margin and Macroscopic Tumor Sites, <https://ClinicalTrials.gov/show/NCT04267575>.
- [41] K. Pefani-Antimisiari, D.K. Athanasopoulos, A. Marazioti, K. Sklias, M. Rodi, A. L. de Lastic, A. Mouzaki, P. Svarnas, S.G. Antimisiaris, Synergistic effect of cold atmospheric pressure plasma and free or liposomal doxorubicin on melanoma cells, *Sci. Rep.* 11 (1) (2021), 14788, <https://doi.org/10.1038/s41598-021-94130-7>.
- [42] V. Vijayarangan, A. Delalande, S. Dozias, J.M. Pouvesle, E. Robert, C. Pichon, New insights on molecular internalization and drug delivery following plasma jet exposures, *Int. J. Pharm.* 589 (2020), 119874, <https://doi.org/10.1016/j.ijpharm.2020.119874>.
- [43] Y. Terada, J. Ogura, T. Tsujimoto, K. Kuwayama, T. Koizumi, S. Sasaki, H. Maruyama, M. Kobayashi, H. Yamaguchi, K. Iseki, Intestinal P-glycoprotein expression is multimodally regulated by intestinal ischemia-reperfusion, *J. Pharm. Pharmaceut. Sci.* 17 (2) (2014) 266–276, <https://doi.org/10.18433/j3jg7d>.